

## Supplementary Figures and Legends

**Supplemental Fig. 1.** Negative controls show the specificity of co-immunoprecipitation of CaMKII and NR2. Triton X-100-insoluble fraction (TIF) of rat hippocampus were immunoblotted (lane 1, input, 20  $\mu$ g) and immunoprecipitated (200  $\mu$ g) by various agents, including p-CaMKII antibody (lane 2), CaMKII antibody (lane 3), a non-specific IgG (NS-IgG; lane 4 and 5) and bead of protein A (lane 6). Blots were probed for NR 2A (up), NR2B (middle) and CaMKII (bottom).

**Supplemental Fig. 2.** PKC activation by physiological stimuli elicited NMDARs insertion which also required CaMKII activity. *A*, Persistent enhancement of NMDAR function induced by theta-burst stimulation (TBS; five trains of burst with four pulses at 100 Hz, at 200 ms interval, repeated four times at intervals of 10 s; for reference, see 30) was abolished by either CaMKII antagonist Myr-AIP (1  $\mu$ M) or exocytosis blocker tetanus toxin (TeTx, 0.1  $\mu$ M), suggesting NMDAR exocytosis accounts for the enhancement of NMDAR function and requires CaMKII activity (TBS:  $1.68 \pm 0.05$ ,  $n = 4$ , compared with baseline  $p < 0.001$ ; Myr-AIP:  $1.06 \pm 0.03$ ,  $n = 4$ ,  $p < 0.001$ ; TeTx:  $0.96 \pm 0.01$ ,  $n = 4$ ,  $p < 0.001$ ). *B*, Statistical plots of data from experiments such as shown in (*A*). \*\*\* $p < 0.001$  compared within indicated groups. *C*, TBS elicited PKC phosphorylation and concurrent potentiation in CaMKII autophosphorylation and postsynaptic NR2 subunit expression (NR2A:  $1.54 \pm 0.21$ ,  $n = 5$ ,  $p < 0.05$ ; NR2B:  $1.47 \pm 0.23$ ,  $n = 5$ ,  $p < 0.05$ ; p-PKC:  $1.72 \pm 0.28$ ,  $n = 5$ ,  $p < 0.05$ ; p-CaMKII:  $1.48 \pm 0.22$ ,  $n = 5$ ,  $p < 0.05$ ). This potentiation could be abolished by CaMKII antagonist Myr-AIP (1  $\mu$ M), suggesting that the potentiation depends on CaMKII activation (NR2A:  $1.06 \pm 0.19$ ,  $n = 5$ , compared with baseline  $p > 0.05$ ; NR2B:  $1.09 \pm 0.20$ ,  $n = 5$ ,  $p > 0.05$ ; p-PKC:  $0.97 \pm 0.21$ ,  $n = 5$ ,  $p < 0.05$ ; p-CaMKII:  $1.05 \pm 0.21$ ,  $n = 5$ ,  $p > 0.05$ ). *D*, Statistical plots of data from experiments such as shown in (*C*). \* $p < 0.05$  compared with control, one-way ANOVA LSD test.

**Supplemental Fig. 3.** Without PKC activation both Tat-NR2 peptides failed to display obvious effects on NMDAR or AMPAR-mediated synaptic responses. Tat-NR2A or Tat-NR2B peptides did not display any obvious effects on NMDA EPSCs amplitude (*A*, Tat-NR2A:  $0.97 \pm 0.11$ ,  $n = 4$ , compared with baseline  $p > 0.05$ ; Tat-NR2B:  $0.97 \pm 0.14$ ,  $n = 4$ ,  $p > 0.05$ ) or decay time (*B*, Tat-NR2A:  $0.94 \pm 0.15$ ,  $n = 4$ ,  $p > 0.05$ ; Tat-NR2B:  $1.01 \pm 0.17$ ,  $n = 4$ ,  $p > 0.05$ ). *C*, Both Tat-NR2 peptides failed to AMPAR-mediated synaptic responses (AMPA-EPSCs, Tat-NR2A:  $1.04 \pm 0.03$ ,  $n = 4$ ,  $p > 0.05$ ; Tat-NR2B:  $0.99 \pm 0.02$ ,  $n = 4$ ,  $p > 0.05$ ).

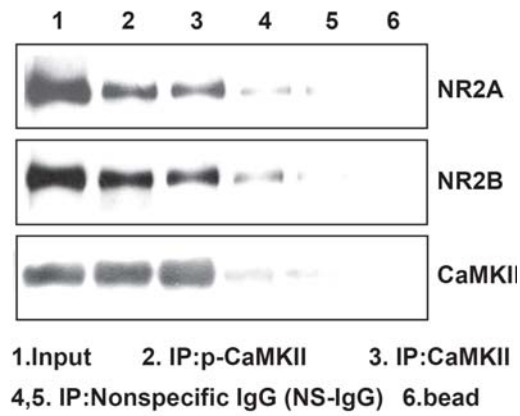
**Supplemental Fig. 4.** Both Tat-NR2 peptides blocked the induction of LTP mediated by the paired-stimulations (200 synaptic stimuli at 2 Hz during a 2.5 min depolarization to 0 mV; Tat-NR2A:  $0.98 \pm 0.01$ ,  $n = 7$ , compared with baseline  $p > 0.05$ ; Tat-NR2B:  $0.94 \pm 0.02$ ,  $n = 6$ ,  $p > 0.05$ ), whereas scrambled Tat-peptide failed to display any obvious effect on LTP (scrambled Tat-peptide:  $1.86 \pm 0.09$ ,  $n = 4$ , compared with LTP  $p > 0.05$ ).

**Supplemental Fig. 5.** Marked increase in the expression of PKC expression upon PKC activation. *A*, PKC activation by PMA treatment markedly increased postsynaptic expression of PKC. This enhancement was totally antagonized by the specific PKC antagonist chelerythrine chloride (Che, 10  $\mu$ M), but was not affected by the CaMKII antagonist Myr-AIP (1  $\mu$ M). *B*, Statistical plot of data showing the effects of Myr-AIP and Che on PMA-induced enhancement of PKC expression at postsynaptic sites, as in *A*. \*\* $p < 0.01$  compared with control.

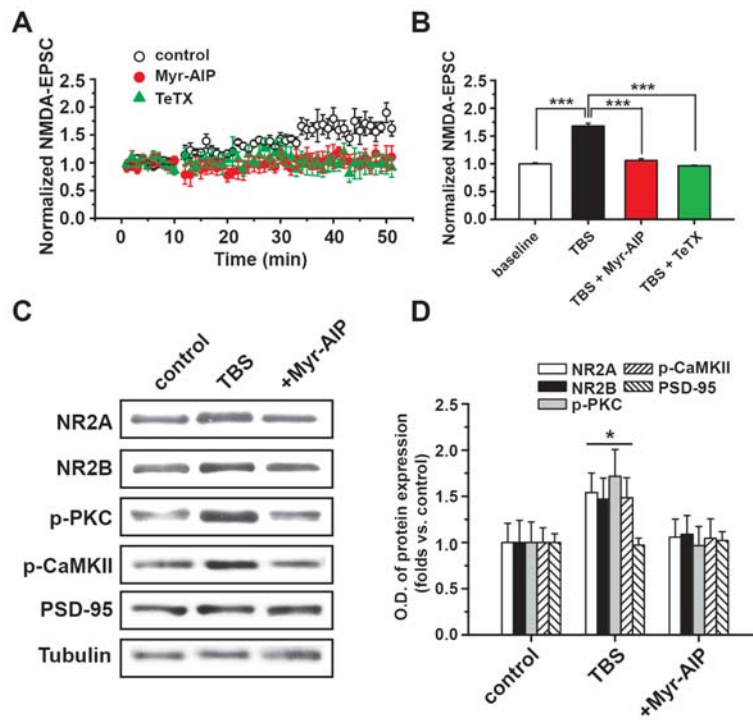
**Supplemental Fig. 6.** Inactive form of CaMKII (heated CaMKII), which was applied through pipette, failed to induce obvious changes in baseline AMPAR-mediated EPSCs ( $n = 5$ ).

**Supplemental Fig. 7.** PMA induces chemical LTP. The potentiation magnitude stabilized after about 20 min ( $n = 5$ ).

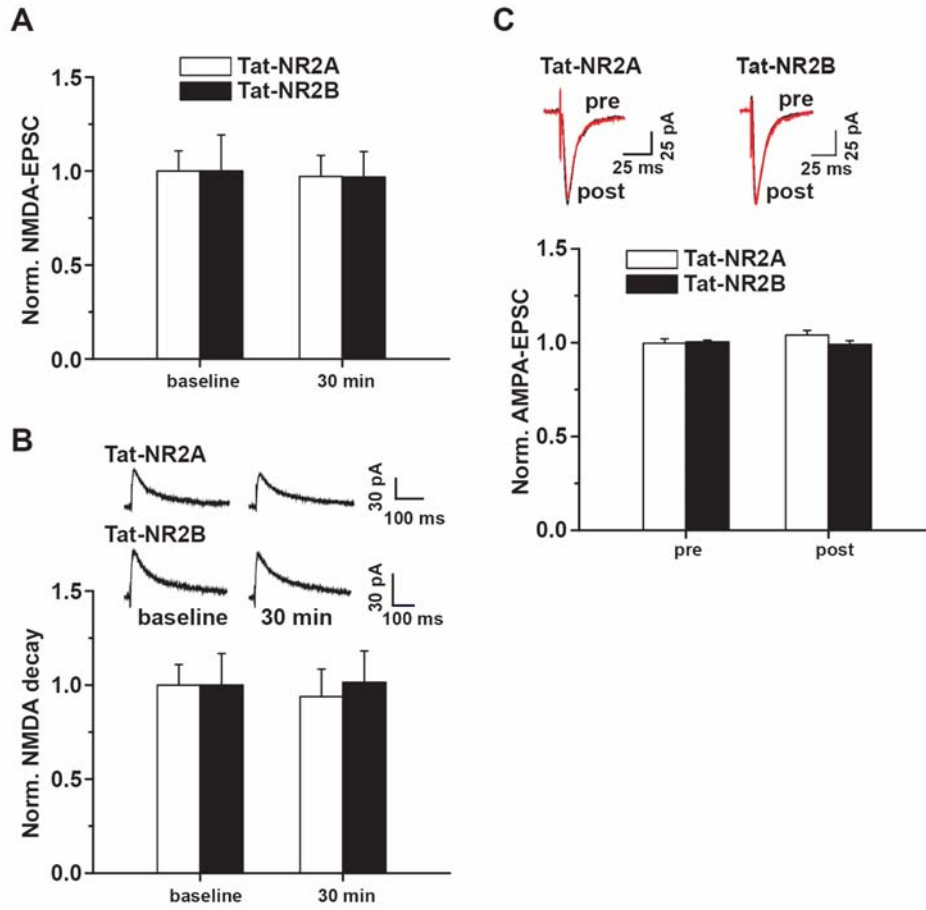
**Supplemental Fig. 8.** A model for differential roles of CaMKII and Src in PKC-induced NMDA potentiation. PKC indirectly triggers CaMKII autophosphorylation and subsequent enhancement of binding between CaMKII and NMDARs in the cytoplasm. As a result, the CaMKII-NR complex translocates to postsynaptic sites through SNARE-dependent exocytosis, which is also regulated by PKC (see Lau et al., 2010; Suh et al., 2010). On the other hand, PKC itself translocates to postsynaptic sites upon PKC activation, where it activates Src family kinases and in turn mediates tyrosine phosphorylation of NMDARs. As a result, the gating of NMDAR channels is significantly enhanced. Therefore, CaMKII and Src independently and partially contribute to PKC-induced NMDAR potentiation through distinct mechanisms. NR, NMDA receptor; CaMKII-NR, CaMKII-NMDAR complex.



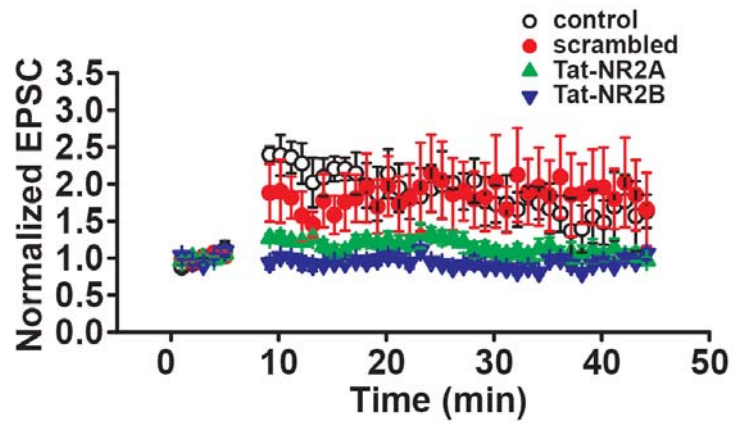
Supplemental Fig. 1. Yan *et al.*



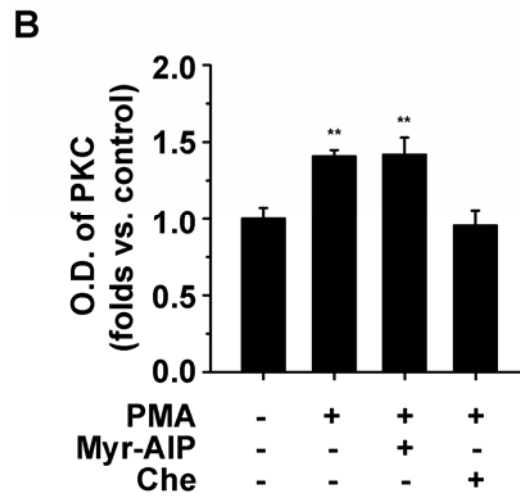
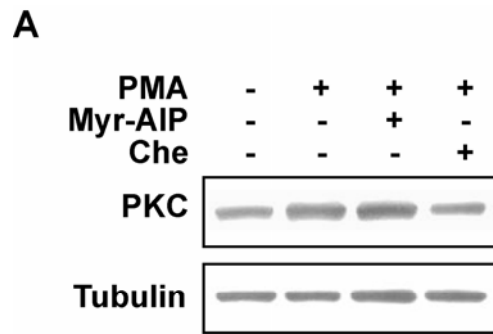
Supplemental Fig. 2. Yan *et al.*



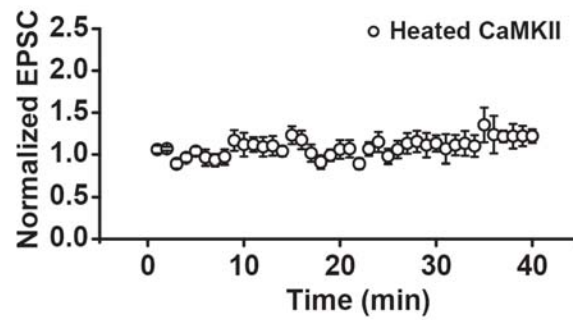
Supplemental Fig. 3. Yan *et al.*



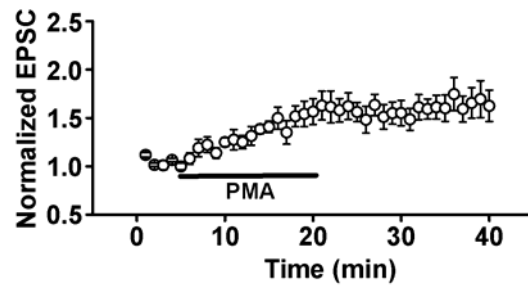
Supplemental Fig. 4. Yan *et al.*



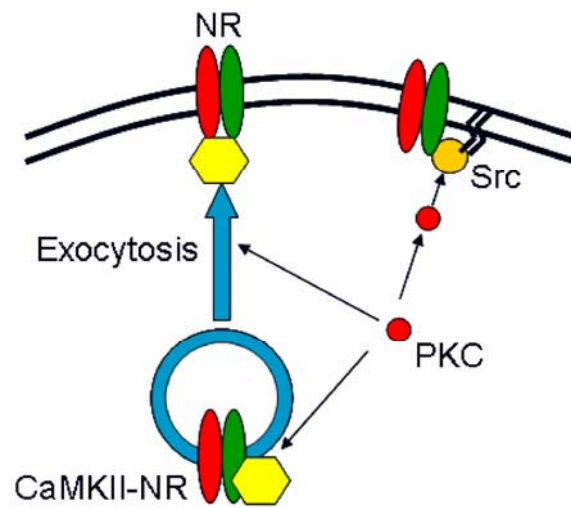
Supplemental Fig. 5. Yan *et al.*



Supplemental Fig. 6. Yan *et al.*



Supplemental Fig. 7. Yan *et al.*



Supplemental Fig. 8. Yan *et al.*